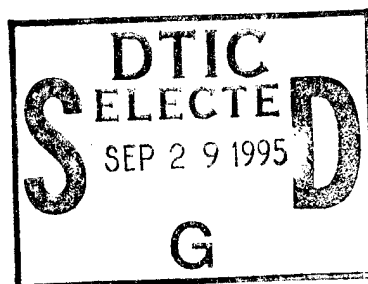ARMY RESEARCH LABORATORY

Acceleration Sensitivity and Mode Shape Relationship Tests of Voltage Controlled Surface Acoustic Wave Oscillator

Jeffrey Himmel, John Gualtieri and John Kosinski

ARL-TR-433

DTIC
SELECTED
SEP 2 9 1995
G

August 1995

19950927 058

DTIC QUALITY INSPECTED 5

NOTICES

Disclaimers

REPORT DOCUMENTATION PAGE		*Form Approved* *OMB NO. 0704-0188*

1. AGENCY USE ONLY *(Leave blank)*	2. REPORT DATE August 1995	3. REPORT TYPE AND DATES COVERED Final Report: Jan 95 to Jun 95	

4. TITLE AND SUBTITLE
ACCELERATION SENSITIVITY AND MODE SHAPE RELATIONSHIP TESTS OF VOLTAGE CONTROLLED SURFACE ACOUSTIC WAVE OSCILLATOR

5. FUNDING NUMBERS

6. AUTHOR(S)
Jeffrey Himmel, John Gualtieri and John Kosinski

7. PERFORMING ORGANIZATION NAMES(S) AND ADDRESS(ES)
US Army Research Laboratory (ARL)
Physical Sciences Directorate (PSD)
ATTN: AMSRL-PS-ED
Fort Monmouth, NJ 07703-5601

8. PERFORMING ORGANIZATION REPORT NUMBER

ARL-TR-433

9. SPONSORING / MONITORING AGENCY NAME(S) AND ADDRESS(ES)

10. SPONSORING / MONITORING AGENCY REPORT NUMBER

11. SUPPLEMENTARY NOTES

12a. DISTRIBUTION / AVAILABILITY STATEMENT

Approved for public release; distribution is unlimited.

12 b. DISTRIBUTION CODE

13. ABSTRACT *(Maximum 200 words)*
Acceleration sensitivity continues to be a significant problem is SAW oscillators. Reducing acceleration sensitivity of SAW oscillators requires an understanding of the nature and causes of acceleration sensitivity. One aspect of this is the correlation between acceleration sensitivity and the transverse mode behavior of SAW resonators. This report discusses the experimental investigation of such a correlation. A 98.5 MHz SAW resonator, for which the transverse modes have been previously measured at various frequencies, was mounted in a VCO and submitted to acceleration sensitivity tests at the frequencies of known transverse mode behavior. The VCO was designed in-house specifically for this investigation. The experimental results indicate that the acceleration sensitivity of SAW resonators does not strongly depend on the transverse mode behavior.

14. SUBJECT TERMS
Acceleration senistivity; mode shape; surface acoustic wave oscillator; voltage controlled oscillator

15. NUMBER IF PAGES
35

16. PRICE CODE

17. SECURITY CLASSIFICATION OR REPORT Unclassified	18. SECURITY CLASSIFICATION OF THIS PAGE Unclassified	19. SECURITY CLASSIFICATION OF ABSTRACT Unclassified	20. LIMITATION OF ABSTRACT UL

Contents

Figures

Tables

Accesion For		
NTIS CRA&I		X
DTIC TAB		☐
Unannounced		☐
Justification		
By		
Distribution /		
Availability Codes		
Dist	Avail and / or Special	
A-1		

iv

Introduction

Surface acoustic wave (SAW) oscillators serve as key components in many military systems, such as Identification Friend or Foe (IFF) systems on helicopters and tanks, surveillance systems on Unmanned Airborne Vehicles (UAV), smart munitions, etc. However, severe vibrations in the battlefield and on platforms greatly restrict the operation of oscillators, including those using SAW resonators.

SAW oscillators under external vibrations exhibit unwanted phase noise in the form of sidebands, i.e., signals in the frequency domain (signal power versus frequency) on either side of the carrier signal. A SAW resonator is one type of electroded crystal oscillator using a piezoelectric crystal, as described by Ballato [1]. In a piezoelectric material, a change in shape produces an electric potential, and vice versa. This is called the piezoelectric effect. In a piezoelectric oscillator, such as a SAW oscillator, the piezoelectric effect converts an electrical signal into vibration and then converts that vibration back into an electrical signal. External vibrations are also converted to an electrical signal. If a resonator operates at its resonant frequency, f_r, and if external vibrations are applied at a frequency f_v that is much less than f_r, then sidebands will exist at $f_r + f_v$ and $f_r - f_v$.

Vibration-induced sidebands cause significant oscillator phase noise which may exceed the total allowable system phase noise [2]. This seriously reduces the effectiveness of military systems and makes it necessary to design oscillators and resonators to have the lowest possible sensitivity to environmental vibrations.

Most SAW oscillators have acceleration sensitivities exceeding 1×10^{-9} /g [3]. Present and future military applications will require an acceleration sensitivity on the order of 10^{-12} /g.

It has been suggested by Ballato, et al. [4], that acceleration sensitivity may be altered by adjusting the "mode shape" in the SAW resonator. The term "mode shape" refers to the standing wave pattern of stress and strain which is induced in a SAW resonator during oscillation. The transverse profile of the acoustic standing wave is a function of the frequency of operation. Thus, when the frequency of operation is altered, the mode shape is altered, which may alter the acceleration sensitivity.

In order to investigate the relationship between acceleration sensitivity and transverse mode shape, a SAW resonator, for which the transverse modes have been previously identified with regard to their spatial distribution [5], was mounted in a VCO and submitted to acceleration sensitivity tests. The VCO can be operated at any frequency within a 300 kHz bandwidth centered about 98.5 MHz. The tests were conducted at specific frequencies at which the transverse mode profile was known.

Design of the 98.5 MHz VCO

There are two criteria necessary for an oscillator to operate. An integral number of wavelengths at the desired frequency must fit in the oscillation loop. Also, the gain in the oscillation loop must be at least as large as the losses around the oscillation loop. In the 98.5 MHz VCO, the first criterion was met by an electronic phase shifter which uses diodes to vary the phase, as will be elaborated shortly. In meeting the second criterion, enough amplification was placed in the oscillation loop to provide the gain necessary to sustain oscillation. However, in order to allow for future testing of other resonators with possibly much higher insertion loss, two extra amplifiers were placed in the circuit, bringing the total number of amplifiers to three. It is a good rule of thumb to keep the excess loop gain below 5 dB so that an excessively high noise floor is prevented. In the VCO, this was achieved by providing space in the circuit for attenuators. The actual gain of the amplifiers usually differs slightly from the nominal gain advertised by the manufacturer. Thus, the amount of attenuation placed in the oscillation loop depended on the actual gain measured in the circuit.

The available 98.5 MHz two-port SAW resonator was designed and fabricated at ARL and will be referred to here as ARL/PSD SAW-1. After its transverse mode behavior had been measured, its loss curve and phase curve were measured on a Hewlett Packard 8510B network analyzer. **Figure 1** and **Figure 2** show the loss curve and phase curve of ARL/PSD SAW-1. The frequencies at which the mode shapes have been measured are indicated in **Figure 1**. **Figure 3** illustrates the mode shapes measured using the apparatus described in reference [5]. **Figure 4** shows a schematic diagram of the VCO that was designed for the resonator.

The dimensions of the power splitter, attenuators and SAW resonator are shown in **Figure 5**.

A typical electronic phase shifter is illustrated in **Figure 6**. The phase shifter shown is basically a T-section high pass filter in which the varactor diodes serve as variable capacitors. The cutoff frequency and transmission phase shift are varied by changing the capacitance of the two varactor diodes, which is done by varying the D.C. bias to the varactor diodes. This, in turn, varies the frequency of oscillation within the passband of the resonator. The varactor diode junction capacitance and the inductance are chosen so that the nominal cutoff frequency is at the center of the operating range. They are given by:

$$L_1 = \frac{R_0}{(2\pi f_0)} \qquad (1)$$

and

$$C_J(V_{MR}) = \frac{1}{(2\pi f_0 R_0)}, \qquad (2)$$

where L_1 is the inductance, R_0 is the characteristic impedance of the system, $C_J(V_{MR})$ is the varactor's capacitance at the center of the voltage tuning range, V_{MR} is the voltage corresponding to the center of the voltage tuning range, and f_0 is the nominal center of the operating frequency range [6] . In **Figure 6**, V_{tune} is the tuning voltage, R_1 is the bias resistance, C_c is for coupling, and C_B is the bypass capacitor. The phase shifter shown in **Figure 6** is called a phase-shifter stage. In order to increase the phase shift, two or more phase-shifter stages can be cascaded.

In the application at hand, $f_0 = 98.5 \times 10^6$ Hz and $R_0 = 50\ \Omega$. When applied to Equations (1) and (2), these resulted in $L_1 = 80.8$ nH and $C_J(V_{MR}) = 23$ pF as the desired values. The available inductor with the closest value to the desired value had an inductance of $L_1 = 69$ nH.

Due to budget constraints, it was decided not to purchase new diodes with known junction capacitance, but to use surplus diodes from previous projects. Available phase shifter test fixtures were used to test the diodes to determine which type would be appropriate, namely, the diode type which would yield the largest phase shift, the largest sensitivity (change in phase shift per change in voltage), and the least attenuation. Each test fixture consisted of a T-section with two diodes as shown in **Figure 6**. In order to find the breakdown voltage and the threshold voltage of each type of diode, the current-voltage curve was measured on a Tektronix Type 576 Curve Tracer. The type of diode chosen was the IN936B. After one pair of these diodes was tested on one fixture, three fixtures were cascaded and three pairs of diodes were used in order to determine the maximum loss and phase shift that would result. **Table 1** and **Figure 7** summarize the measurements of the IN936B diodes on the curve tracer and on the phase shifter test fixtures. With three phase-shifter stages in series, the maximum insertion loss was -3.5 dB at a maximum phase change of 237 degrees.

In the VCO, a three stage phase shifter was designed, as shown in **Figure 4**. The bias resistors (R_1, R_2, R_3 and R_4) and the bypass capacitor, C_{14} , were chosen to block the RF signal from reaching the tuning voltage source. The cutoff frequency was given by

$$f_c = \frac{1}{2\pi R\ C_{14}} = 88.4\ \text{Hz}, \qquad (3)$$

3

where $R = R_1 = R_2 = R_3 = R_4 = 10$ kΩ and $C_{14} = 0.18$ μF (see **Figure 4**).

The type of amplifier chosen was the Mini-Circuits monolithic amplifier model MAR-6. Its specifications are listed in **Figure 8**. This model was chosen for all the amplifiers in the circuit since it had the highest gain available for the frequency range of interest, as well as one of the lowest noise factors (3.0 dB). Its small size was also an attractive feature. The manufacturer recommended a bias voltage of $V_d = 3.5$ volts at pin 3 of the amplifier and a bias current of $I_d = 16$ mA. This was achieved with a voltage supply of 5 volts and a bias resistor of about 100 Ω.

The VCO was designed to be realized as a microstrip circuit on a 10 mil (254 micron) circuit board. Once the nominal gains and losses of the components were known, it was necessary to find the width of the 50 Ω microstrip transmission lines and the width of the bias lines. This was accomplished by using a program called "Ferroelectric Support Software" [7]. In this program, the user enters the width of the desired line into the program, along with the circuit board parameters. The program then provides the transmission line impedance and other useful information. The use of this program, along with the circuit parameters, widths and impedances, is outlined in **Figure 9**. A 50 Ω line was found to have a width of 0.783 mm. It was decided that the impedance of the bias lines be 25 Ω, yielding a width of 2.0 mm. The circuit was designed to be 7.5 cm in width and 14 cm in length.

Fabrication and Test of the VCO

The layout of the circuit was drawn on the Hewlett-Packard "Microwave Design System" CAD package. The layout was then submitted electronically to a Gerber plotter in order that the mask be made. The mask, shown to scale in **Figure 10**, was used in the etching process of the circuit. After the circuit was etched, its ground plane was soldered to a brass plate in order to make the ground plane sturdy and stable.

Components were mounted and soldered into the circuit one at a time, with the gains and losses measured at each step. (The test ports were used for this purpose.) Thus, it was found that the overall gain of the three cascaded amplifiers in the oscillation loop was 53.8 dB. **Table 2** lists the gains and losses of the individual components, as well as the total oscillation loop gain. Notice that it was necessary to introduce 35 dB of attenuation into the loop in order to provide a reasonable excess loop gain of 2.8 dB.

The VCO was measured over the operating range using a Hewlett Packard 8566B spectrum analyzer with the span set to 100 kHz. The results are displayed in **Table 3** and **Figure 11**.

4

Acceleration Sensitivity Tests

The shake table setup for the acceleration sensitivity tests is illustrated in **Figure 12**. The vibration frequency is produced by a waveform generator which feeds the signal into a power amplifier. The amplified signal is fed into the shake table. An accelerometer, placed on the VCO as close as possible to the resonator being tested, feeds the acceleration measurement via a feedback loop into an amplitude servo, which displays the acceleration level. The acceleration level is manually adjusted on the amplitude servo, which, in turn, adjusts the amplification level of the power amplifier.

The oscillator behavior for each test was measured directly using an HP 8566B spectrum analyzer. The measurements included the frequencies and power levels of the carrier signal and the first sideband on either side of the carrier signal. The sidebands induced by external vibrations were located at the carrier frequency plus or minus the vibration frequency, in agreement with frequency modulation theory [8] . In order to easily recognize the sidebands, the spectrum analyzer display was set on a span of four times the vibration frequency. Thus, the width of the display screen was divided into four quarters. The carrier signal was placed in the center of the display, so that the first lower sideband was located in the first quarter of the screen width and the first upper sideband was located at the third quarter.

Most of the vibrations experienced by electronic equipment in the battlefield are at 5000 Hz or less. The vibrations are especially concentrated at below 1 kHz due to such vibration sources as tank engines, truck engines, helicopters engines, etc. Thus, vibration frequencies for the acceleration sensitivity tests were chosen with this in mind. However, in order to avoid 60 Hz noise from the wall power outlets in the laboratory, vibration frequencies must not be multiples of 60 Hz. Thus, each vibration frequency was a multiple of 60 Hz plus 20 or 30 Hz. The vibration frequencies at which the tests were conducted were 90, 270, 500, 990, 2370 and 5000 Hz.

The upper and lower sidebands were averaged and put in units of dBc with the following equation:

$$L = \frac{L_{-1} + L_{+1}}{2} - P_0 \qquad (4)$$

where L_{-1} is the power of the first lower sideband in dBm, L_{+1} is the power of the first upper sideband in dBm and P_0 is the carrier power in dBm.

The inverse log of L was taken in order to put it in terms of voltage ratios, as follows:

$$E = 10^{L/20} = \frac{\text{(Voltage Amplitude of 1st sideband)}}{\text{(Voltage Amplitude of carrier)}} \qquad (5)$$

From modulation theory,

$$E = J_1(\beta) / J_0(\beta) \approx 4\beta / (8 - \beta^2) \qquad (6)$$

where $J_1(\beta)$ is the Bessel function of the first kind of order 1, $J_0(\beta)$ is the Bessel of the first kind of order 0, and β is the modulation index [9].

Equation (4) was solved for β.

$$\beta = \frac{[-2 + (4 + 8E^2)^{1/2}]}{E} \qquad (7)$$

The magnitude of the ith component of the acceleration sensitivity vector was given by

$$\Gamma_i = \frac{\beta \cdot f_v}{|A| \cdot f_0}, \qquad (8)$$

where f_v was the vibration frequency in Hz, A was the peak acceleration vector in /g and f_0 was the carrier frequency in Hz [3].

However, in the case of this experiment, the only acceleration sensitivity vector component present was in the vertical direction, i.e., normal to the surface of the VCO and SAW resonator. Thus, to find the magnitude of the acceleration sensitivity vector, it was only necessary to modify Equation (8) slightly as follows:

$$\Gamma_i = \frac{\beta f_v}{|A| f_0}. \qquad (9)$$

The acceleration applied was 1 g in the vertical direction. In other words, $|A| = 1$ g.

At each vibration frequency, measurements were taken at VCO carrier frequencies in the SAW resonator passband where the transverse mode profile was known. The carrier frequency of the VCO was varied by adjusting the tuning voltage in the range of about 1.6 volts to about 5.6 volts.

The results of the acceleration sensitivity tests are presented in **Figures 13** through **18**.

Discussion of Results

Each plot of acceleration sensitivity versus carrier frequency is flat and linear. For example, at a vibration frequency of 90 Hz, the acceleration sensitivity only varies between 8.639×10^{-9} to 9.258×10^{-9} /g (see **Figure 13**). This kind of small variation is seen in all of the results. Thus, the results suggest that the acceleration sensitivity does not strongly depend on the transverse mode behavior.
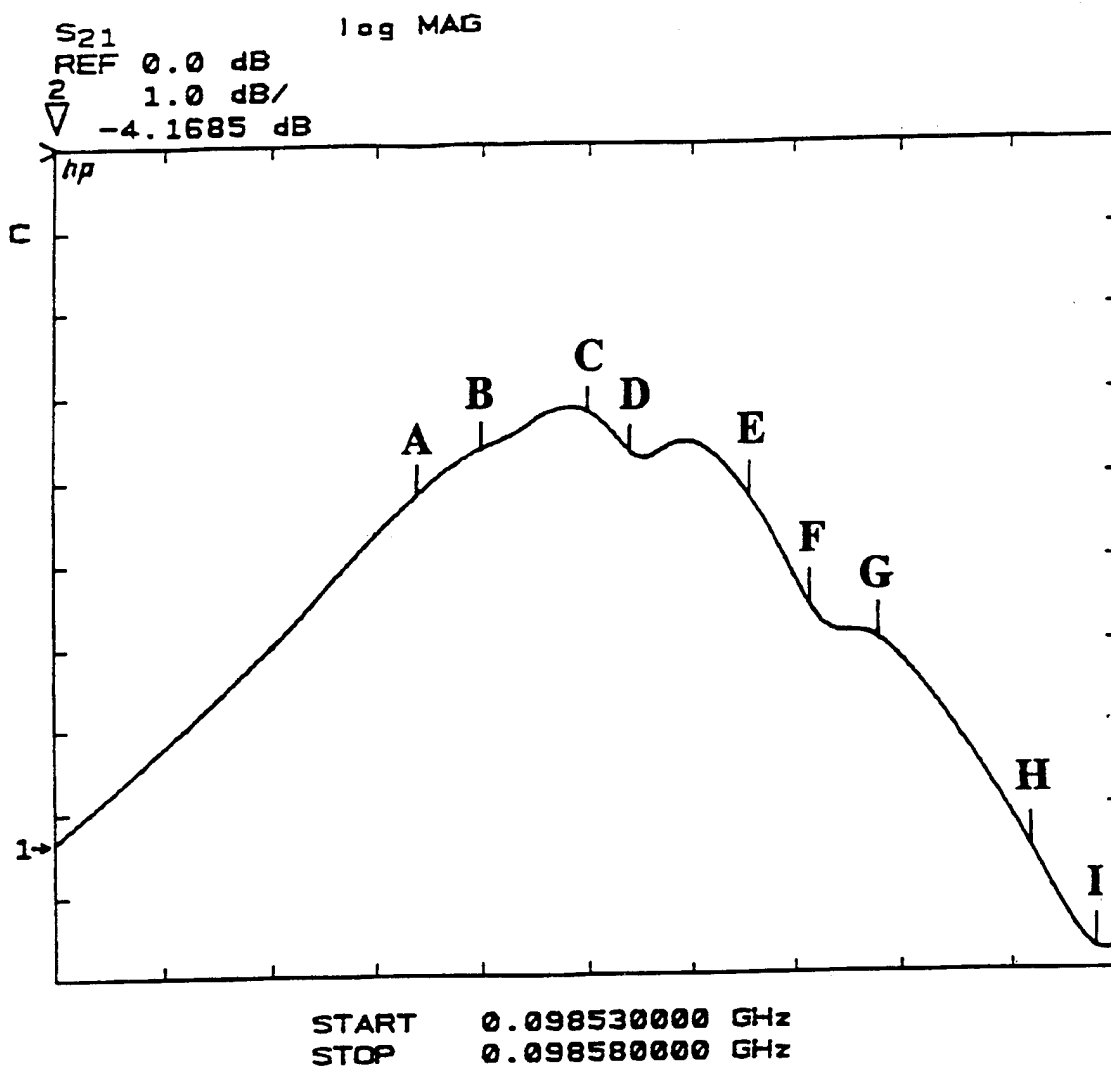
Acknowledgments

References

[1] B. Parzen and A. Ballato, "Design of Crystal and Other Harmonic Oscillators," John Wiley & Sons, New York, 1983, ch. 3.

[2] J. Kosinski, A. Ballato, and T. Lukaszek, "Measurements of Acceleration-Induced Phase Noise in Surface Acoustic Wave Devices," Proc. 44th Annual Frequency Control Symposium, pp. 488-492, May 1990.

[3] J. Himmel, R. McGowan, J. Kosinski and T. Lukaszek, "Market Survey of Acceleration-Insensitive SAW Oscillators," Proc. 46th Annual Frequency Control Symposium, pp. 849-860, May 1992.

[4] A. Ballato, J. Kosinski, T. Lukaszek, M. Mizan, R. McGowan and K. Klohn, "Acceleration Sensitivity Reduction in SAW and BAW Resonators by Electronic Means," Proc. IEEE Ultrasonics Symposium, pp. 573-576, 1990.

[5] J. Gualtieri and J. Kosinski, "Large-Area, Real-Time Imaging System for Surface Acoustic Wave Devices," submitted to IEEE Transactions on Instrumentation and Measurement, 1995.

[6] G. K. Montress, "A High Performance, Hybrid Circuit Electronic Phaseshifter," Proceedings of RF Expo East, pp. 231-236, 1989.

[7] T. Koscica, "Ferroelectric Support Software V.16," Electronics Division, Physical Sciences Directorate, U. S. Army Research Laboratory, Fort Monmouth, New Jersey, 1994.

[8] K. S. Shanmugam, "Digital and Analog Communications," John Wiley & Sons, New York, 1979, p. 281.

[9] J. Kosinski and A. Ballato, "Advances in Acceleration Sensitivity Measurement and Modeling," Proc. 46th Annual Frequency Control Symposium, pp. 838-848.

S21
REF 0.0 dB
2   1.0 dB/
▽ -4.1685 dB

hp

C

A B C D E F G H I

1→

START   0.098530000 GHz
STOP   0.098580000 GHz

Frequencies at which the mode shapes have been measured:

Designation	Frequency, MHz	Loss, dB
A	98.547	-4.2
B	98.550	-3.6
C	98.555	-3.2
D	98.557	-3.7
E	98.563	-4.3
F	98.566	-5.6
G	98.569	-6.0
H	98.576	-8.6
I	98.579	-9.8

Figure 1: Loss curve of ARL/PSD SAW-1.

S21
REF -75.0 °
1   20.0 °/
∇   -77.273 °

hp

MARKER 1
    98.5545 MHz

START   0.098530000 GHz
STOP   0.098580000 GHz
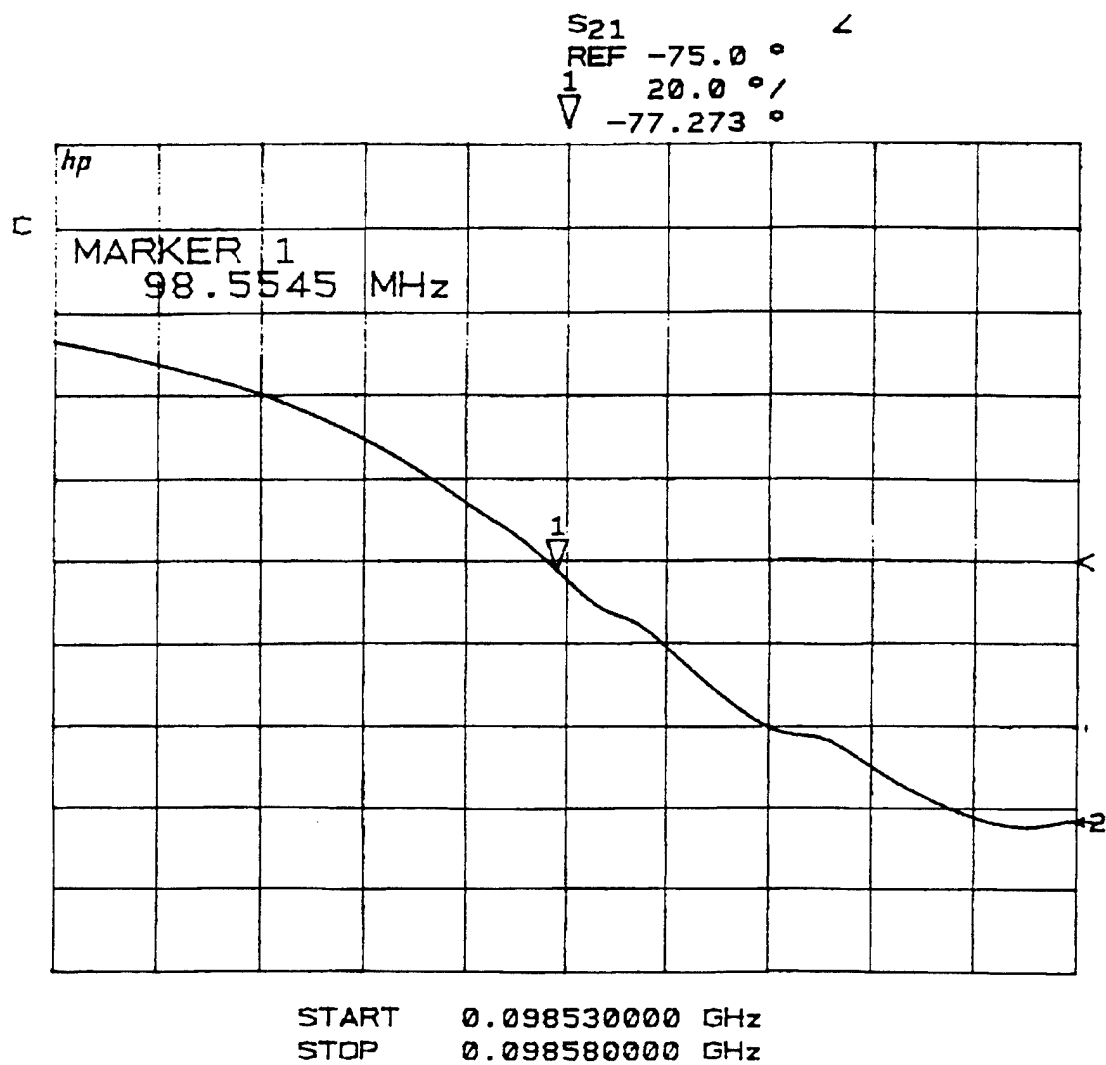
Figure 2: Phase curve of ARL/PSD SAW-1.
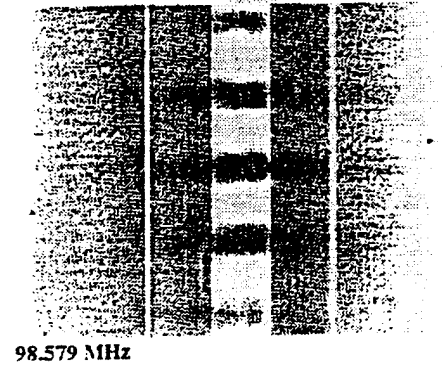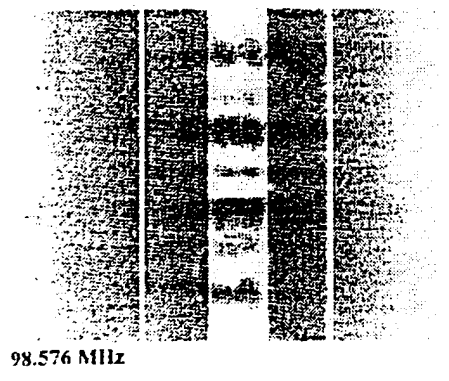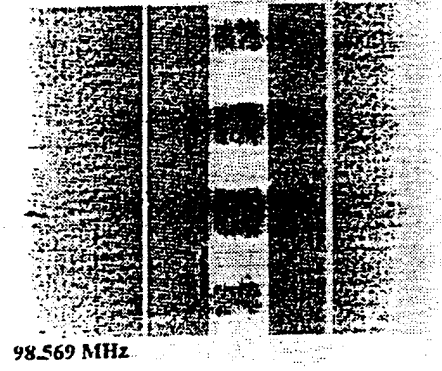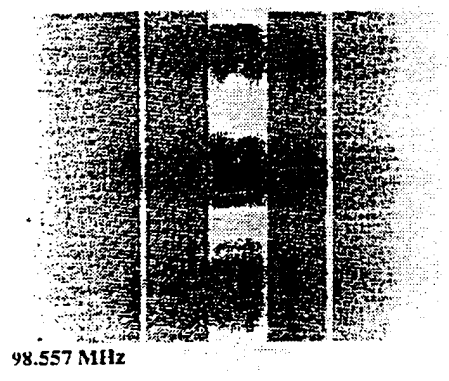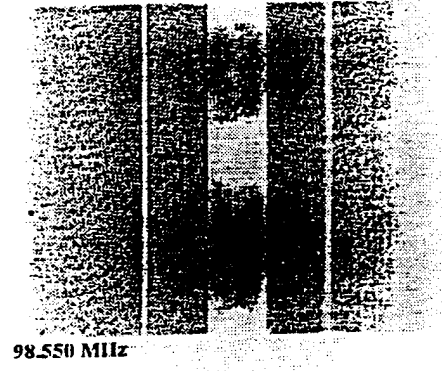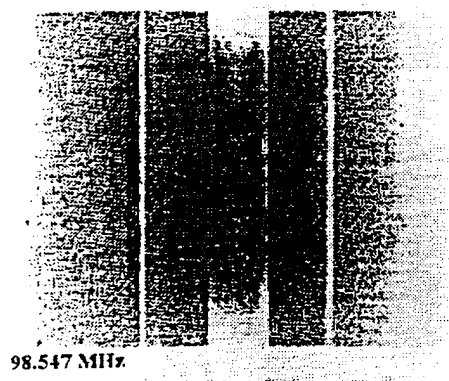
Figure 3: Illustration of the mode shapes of ARL/PSD SAW-1.

Figure 4: Schematic diagram of VCO.
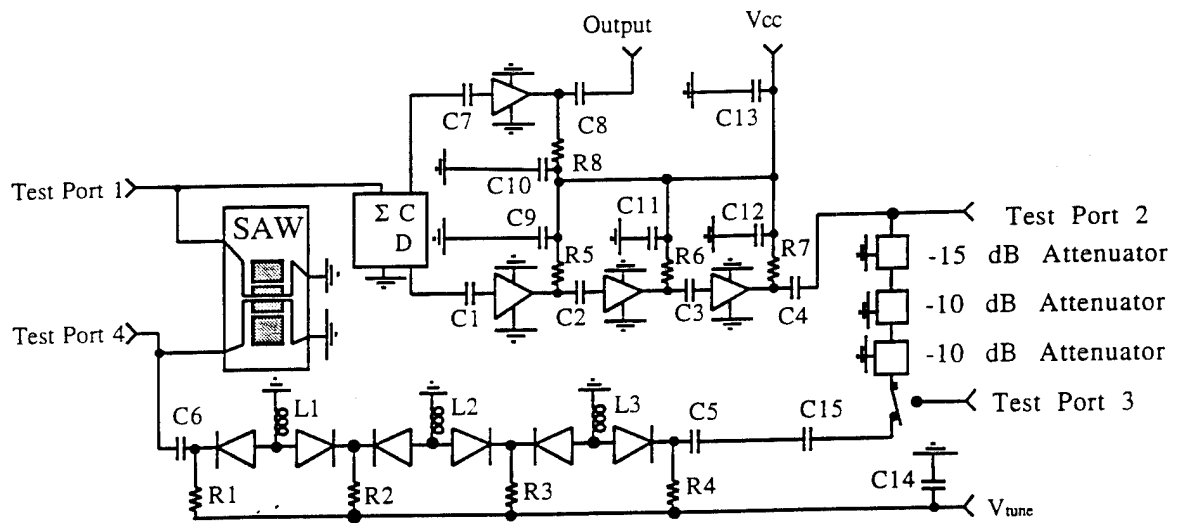
R1 = R2 = R3 = R4 = 10 kΩ

R5 = R6 = R7 = R8 = 100 kΩ

C1 = C2 = C3 = C4 = C5 = C6 = C7 = C8 = C15 = 1000 pF

C9 = C10 = C11 = C12 = 0.47 μF

L1 = L2 = L3 = 69 nH

All diodes are IN936B diodes.

Vcc = 5 volts

Cutoff Frequency for phase shifter bias lines is

$$fc = 1/[(2\pi)(R1)(C14)] = 1/[(2\pi)(10000\ \Omega)(0.18\ F)] = 88.4\ Hz$$

Cutoff Frequency for amplifier bias lines is

$$fc = 1/[(2\pi)(R5)(C9)] = 1/[(2\pi)(100\ \Omega)(0.47\ F)] = 3386.3\ Hz$$
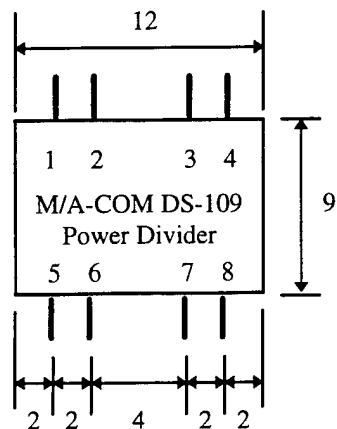
Notes on Power Divider:

Pin 1 is the input and is labeled "Σ" on the case of the power divider. Pin 4 and pin 8 are outputs. Pin 4 is labeled "C" and pin 8 is labeled "D." Pins 2, 3, 5, 6 and 7 are attached to the case and should be grounded.
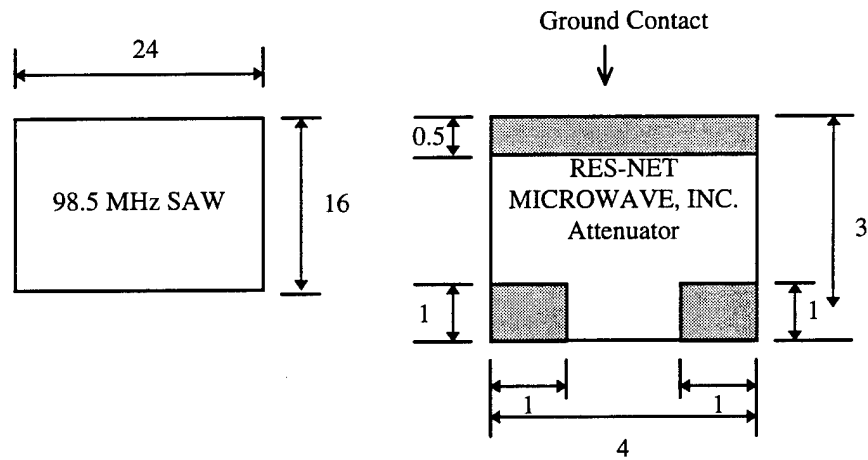
Figure 5: Dimensions of the power splitter, attenuators and the SAW resonator. (Note: These diagrams are not to scale.)

13
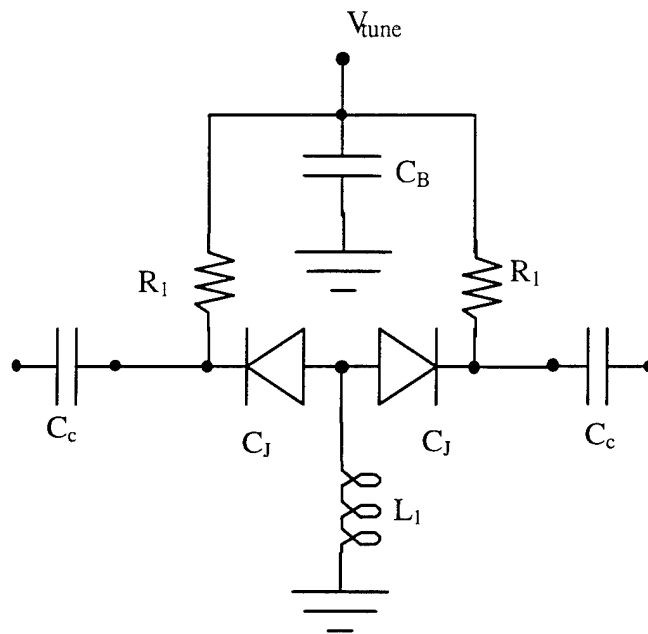
Figure 6: A typical electronic phase shifter.

Measured at 98.6 MHz
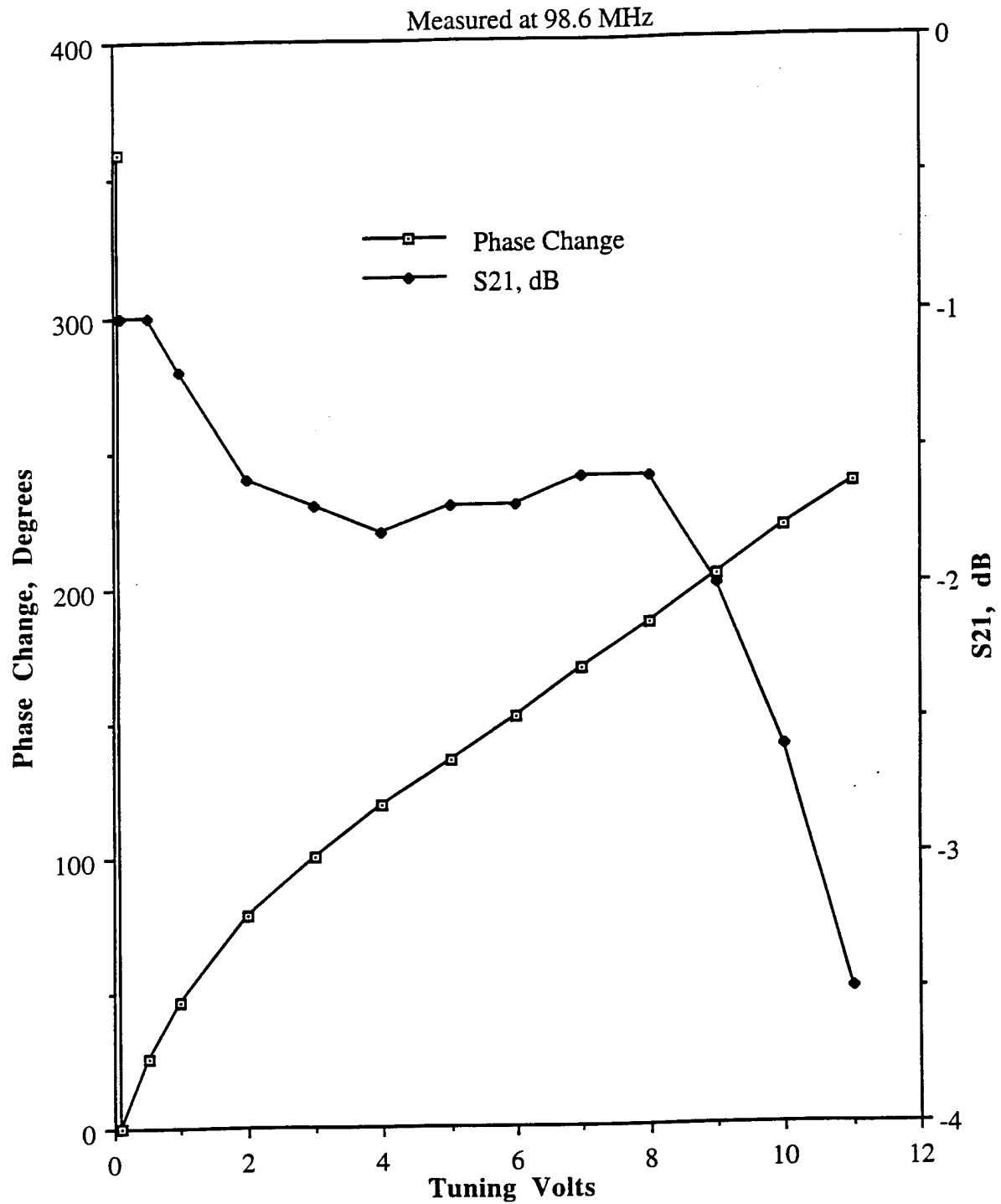
Figure 7: Phase change and S21 versus tuning voltage of the 3-stage phase shifter test of the IN936B diodes.

All Units are in mm:

RF
3 OUT

Dot indicates RF input

4   **2**

RF
1 IN

11.68
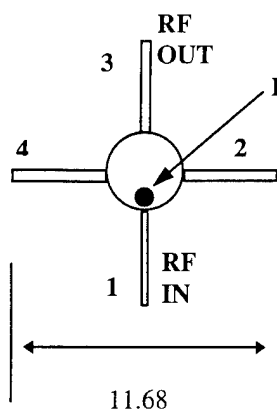
Typical Biasing Configuration:

R_{bias} Vcc

4

3

IN o———|(———o 1

V_d OUT

2

1.52

2.16
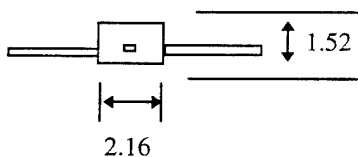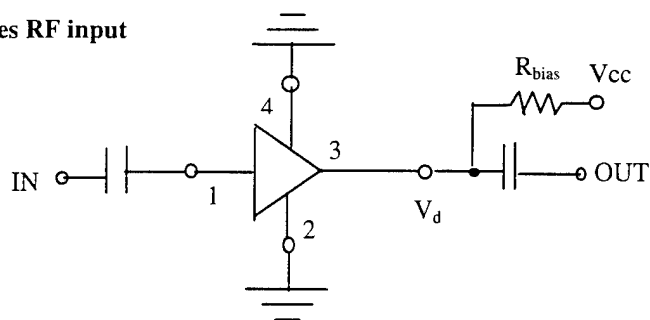
Frequency Range:	DC - 2000 MHz
Gain at 100 MHz:	20 dB
Output at 1 dB Compression:	2.0 dBm
Maximum input without damage:	20 dBm
Noise Factor:	3.0 dB
DC Current at Pin 3:	16 mA = I_d
DC Voltage at Pin 3:	3.5 Volts = V_d

Vcc, volts	$V_{cc} - V_d$	$R_{bias} = (V_{cc} - V_d) / I_d$
5	5 volts - 3.5 volts = 1.5 volts	9.4 Ω
		The closest to this available was 100 Ω.

Figure 8: Specifications of the Mini-Circuits amplifier model MAR-6.
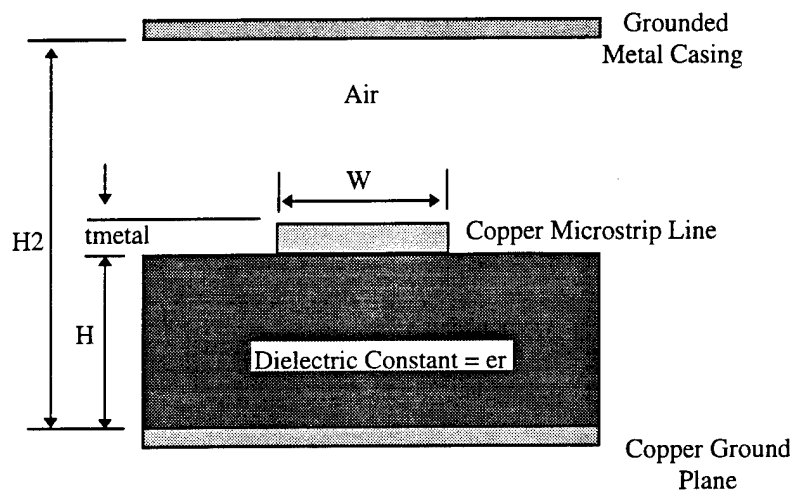
Input Parameters (with Units Used When Entered into the Program):

$$F = 0.0985 \text{ GHz} = \text{Frequency of Operation}$$
$$H = 254 \ \mu m$$
$$H2 = 1.0E6 \ \mu m$$
$$W = 783.836 \ \mu m$$
$$tmetal = 10 \ \mu m$$
$$er = 2.2$$

Output:

$$Z0 = 50 \ \Omega$$

Figure 9: Illustration of the use of the program "Ferroelectric Support Software," along with the circuit parameters, widths and impedances of a 50 ohm line. The diagram shows the cross-sections of the circuit board and top of the metal casing.
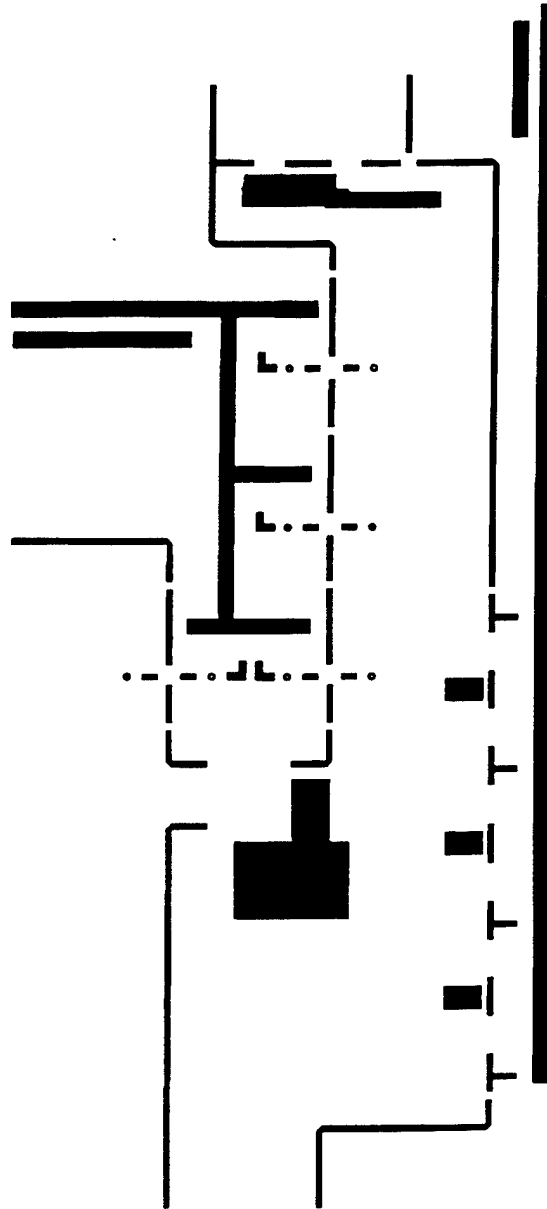
Figure 10: Copy of the mask of the VCO, shown to scale.

18
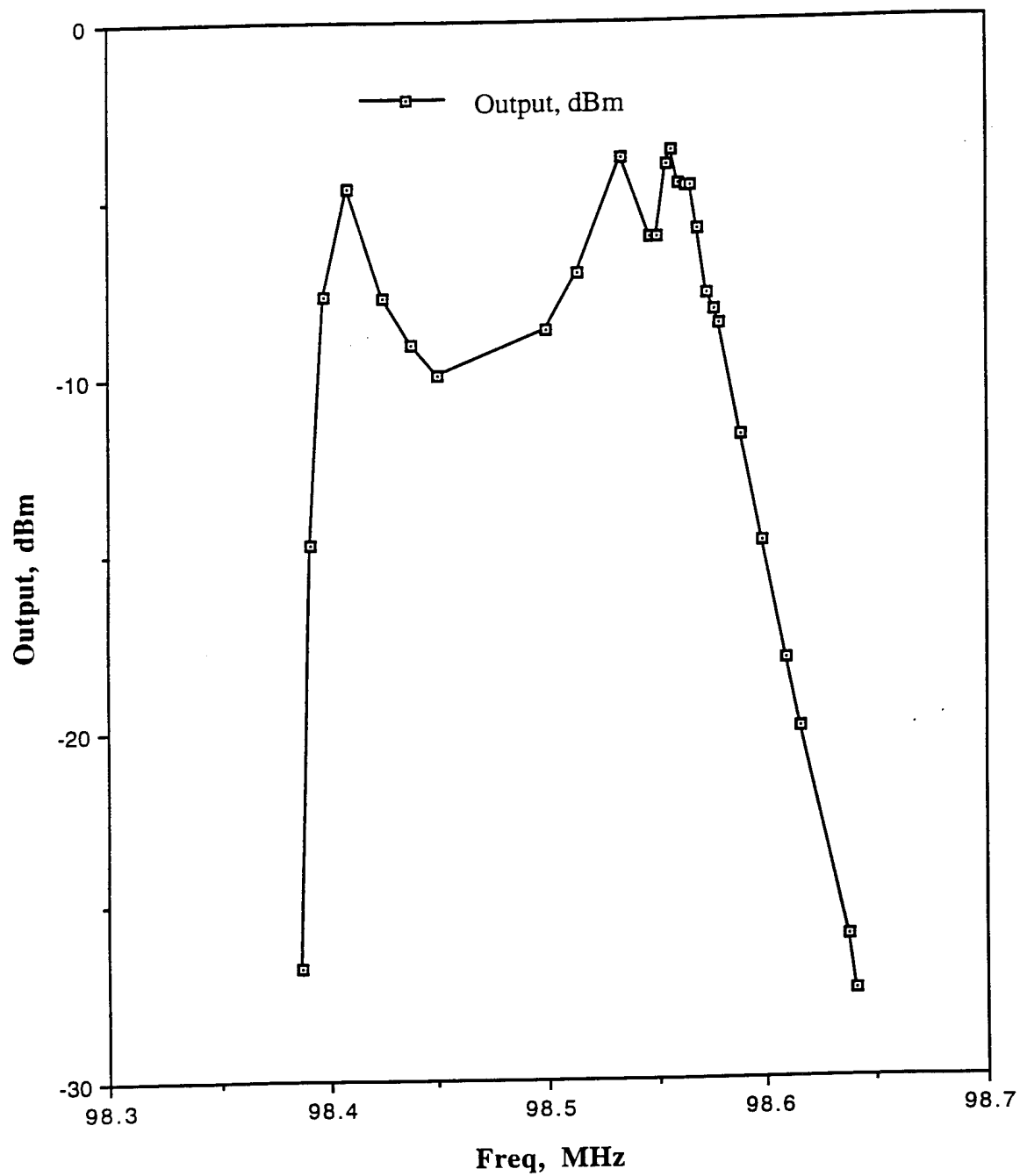
Figure 11: VCO output in dBm versus frequency.
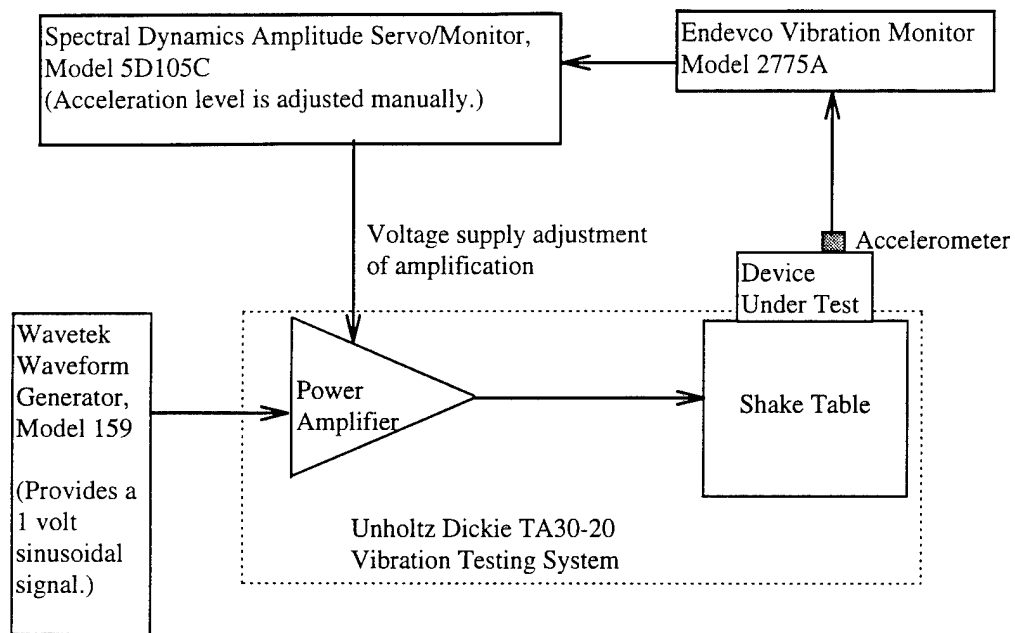
Figure 12: Block diagram of the shake table system.

Acceleration Sensitivity Vs. Frequency
Vibration Frequency = 90 Hz
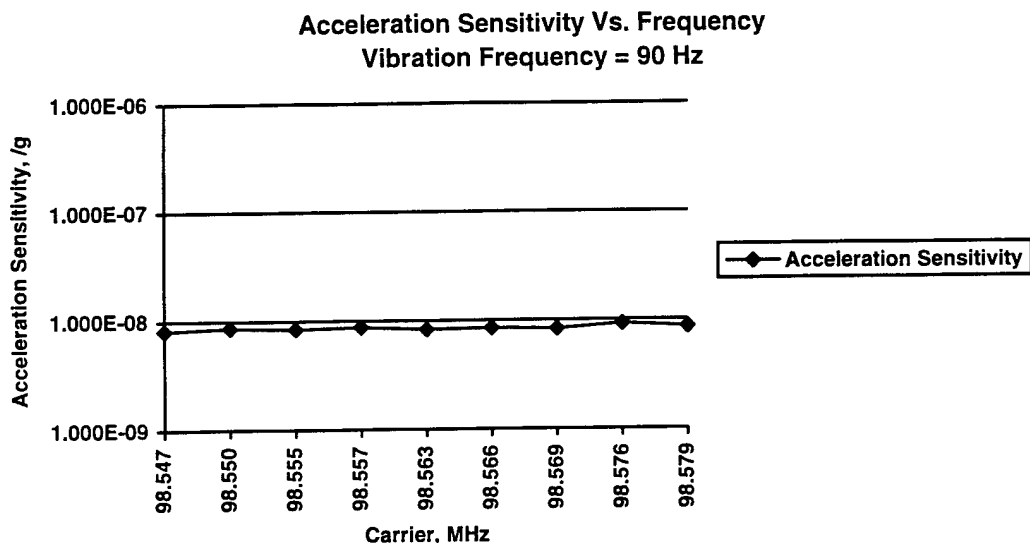
Data:

V$_{tune}$	f$_0$	P$_0$	f$_{+1}$	L$_{+1}$	f$_{-1}$	L$_{+1}$	Γ
1.870	98 547 191.6	-5.90	98 547 283.4	-52.80	98 547 100.5	-52.80	8.253×10^{-9}
2.920	98 550 052.8	-5.70	98 550 142.8	-52.30	98 549 962.4	-52.00	8.692×10^{-9}
4.28	98 555 073.2	-3.70	98 555 163.2	-50.40	98 554 980.7	-50.40	8.445×10^{-9}
4.61	98 557 058.8	-3.60	98 557 148.8	-50.00	98 556 968.4	-50.00	8.741×10^{-9}
4.98	98 563 043.4	-4.30	98 563 138.1	-51.30	98 562 955.9	-50.00	8.347×10^{-9}
5.22	98 566 069.7	-4.50	98 566 152.6	-51.10	98 565 968.3	-51.10	8.542×10^{-9}
5.37	98 569 154.0	-5.70	98 569 246.2	-52.60	98 569 064.4	-52.10	8.347×10^{-9}
5.51	98 576 338.3	-7.80	98 576 429.0	-53.40	98 576 247.9	-54.00	9.258×10^{-9}
5.61	98 579 028.7	-8.30	98 579 119.4	-54.90	98 578 940.5	-54.70	8.639×10^{-9}

Key:

V$_{tune}$ = Tuning Voltage in Volts
f$_0$ = Carrier Frequency in Hz
P$_0$ = Carrier Power in dBm
f$_{+1}$ = First Upper Sideband Frequency in Hz
L$_{+1}$ = First Upper Sideband Power in dBm
f$_{-1}$ = First Lower Sideband Frequency in Hz
L$_{-1}$ = First Lower Sideband Power in dBm
Γ = Calculated Acceleration Sensitivity in g^{-1}

Figure 13: **Results of the acceleration sensitivity tests on the VCO for vibration frequency of 90 Hz. The spectrum analyzer Span was 360 Hz.**

Acceleration Sensitivity Vs. Frequency
Vibration Frequency = 270 Hz
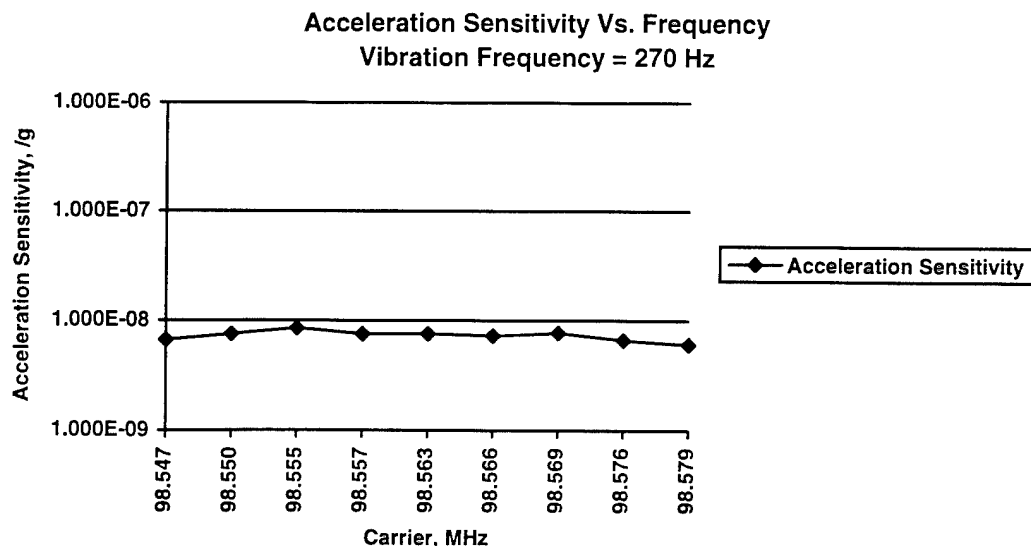
Data:

V_{tune}	f_0	P_0	f_{+1}	L_{+1}	f_{-1}	L_{+1}	Γ
1.835	98 547 026	-5.90	98 547 304	-64.20	98 546 752	-58.30	6.664×10^{-9}
2.987	98 550 044	-5.60	98 550 318	-62.80	98 549 769	-57.25	7.520×10^{-9}
4.27	98 555 005	-3.70	98 555 277	-59.60	98 554 733	-56.20	8.486×10^{-9}
4.62	98 557 010	-3.50	98 557 280	-60.70	98 556 737	-57.20	7.563×10^{-9}
5.00	98 563 118	-4.20	98 563 390	-61.40	98 562 851	-57.20	7.563×10^{-9}
5.22	98 566 065	-4.50	98 566 333	-61.90	98 565 794	-57.55	7.264×10^{-9}
5.37	98 569 039	-5.70	98 569 311	-62.30	98 568 766	-57.00	7.738×10^{-9}
5.50	98 576 013	-7.70	98 576 280	-66.30	98 575 733	-58.35	6.624×10^{-9}
5.61	98 579 029	-8.30	98 579 303	-67.60	98 578 794	-59.15	6.041×10^{-9}

Key:

V_{tune} = Tuning Voltage in Volts
f_0 = Carrier Frequency in Hz
P_0 = Carrier Power in dBm
f_{+1} = First Upper Sideband Frequency in Hz
L_{+1} = First Upper Sideband Power in dBm
f_{-1} = First Lower Sideband Frequency in Hz
L_{-1} = First Lower Sideband Power in dBm
Γ = Calculated Acceleration Sensitivity in g^{-1}

Figure 14: Results of the acceleration sensitivity tests on the VCO for vibration frequency of 270 Hz. The spectrum analyzer span was 1080 Hz.

Acceleration Sensitivity Vs. Frequency
Vibration Frequency = 500 Hz
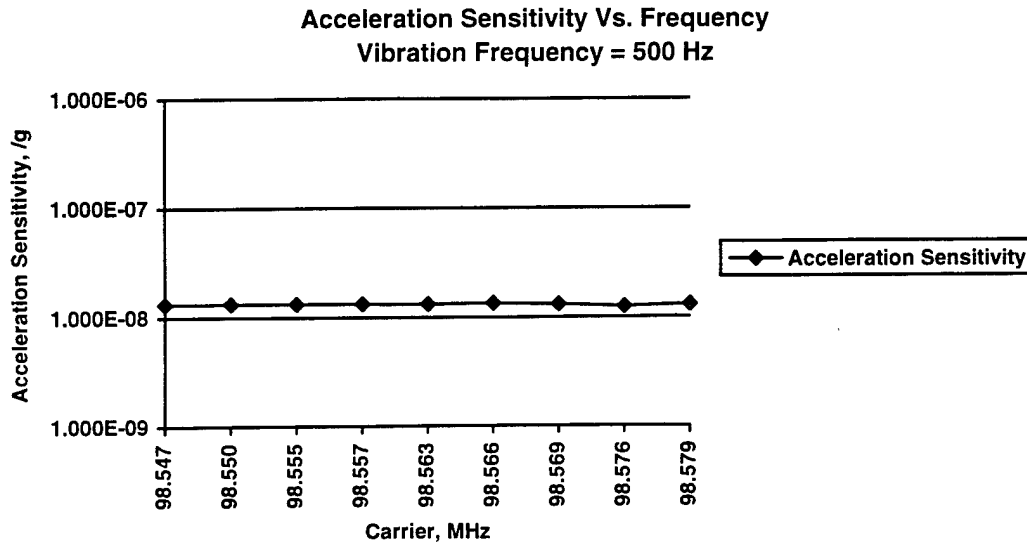
Data:

V_{tune}	f_0	P_0	f_{+1}	L_{+1}	f_{-1}	L_{+1}	Γ
1.884	98 547 050	-5.70	98 547 556	-63.70	98 546 548	-63.10	1.322×10^{-8}
3.01	98 550 040	-5.50	98 550 548	-63.30	98 549 538	-63.00	1.330×10^{-8}
4.36	98 555 034	-3.40	98 555 542	-60.80	98 554 532	-61.20	1.338×10^{-8}
4.68	98 557 006	-3.30	98 557 504	-61.10	98 556 500	-60.70	1.338×10^{-8}
5.03	98 563 108	-4.30	98 563 620	-62.00	98 562 608	-62.00	1.322×10^{-8}
5.26	98 566 015	-4.70	98 566 519	-62.20	98 565 515	-62.20	1.353×10^{-8}
5.41	98 569 031	-6.00	98 569 537	-63.60	98 568 523	-63.90	1.314×10^{-8}
5.51	98 576 036	-8.10	98 576 548	-66.40	98 575 540	-66.10	1.255×10^{-8}
5.63	98 579 040	-8.70	98 579 544	-66.50	98 578 538	-66.60	1.299×10^{-8}

Key:

V_{tune} = Tuning Voltage in Volts
f_0 = Carrier Frequency in Hz
P_0 = Carrier Power in dBm
f_{+1} = First Upper Sideband Frequency in Hz
L_{+1} = First Upper Sideband Power in dBm
f_{-1} = First Lower Sideband Frequency in Hz
L_{-1} = First Lower Sideband Power in dBm
Γ = Calculated Acceleration Sensitivity in g^{-1}

Figure 15: Results of the acceleration sensitivity tests on the VCO for vibration frequency of 500 Hz. The spectrum analyzer span was 2000 Hz.

Acceleration Sensitivity Vs. Frequency
Vibration Frequency = 990 Hz
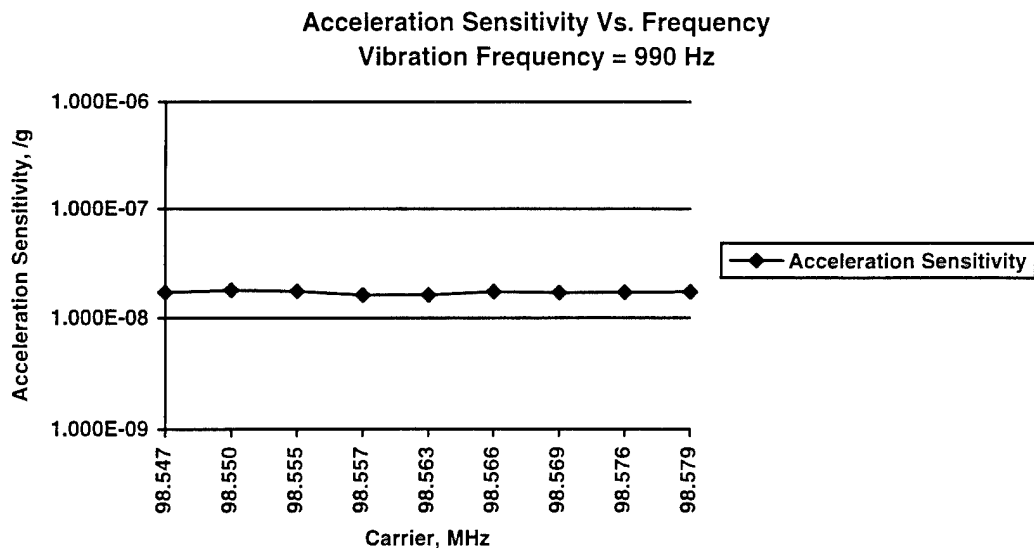
Data:

V_{tune}	f_0	P_0	f_{+1}	L_{+1}	f_{-1}	L_{+1}	Γ
1.710	98 547 037	-6.00	98 548 027	-67.50	98 546 043	-67.30	1.710×10^{-8}
2.886	98 550 018	-5.90	98 551 024	-66.60	98 549 028	-67.10	1.801×10^{-8}
4.26	98 555 019	-3.80	98 556 021	-64.70	98 554 033	-65.20	1.760×10^{-8}
4.63	98 557 002	-3.50	98 557 992	-65.30	98 556 016	-65.40	1.624×10^{-8}
5.00	98 563 038	-4.60	98 564 028	-66.10	98 562 044	-66.10	1.690×10^{-8}
5.25	98 566 028	-4.80	98 567 018	-65.80	98 565 038	-66.30	1.740×10^{-8}
5.40	98 569 136	-6.20	98 570 126	-67.60	98 568 146	-67.70	1.700×10^{-8}
5.51	98 576 008	-8.20	98 577 006	-69.40	98 575 018	-69.80	1.710×10^{-8}
5.63	98 579 004	-8.80	98 579 998	-70.00	98 578 002	-70.20	1.729×10^{-8}

Key:

V_{tune} = Tuning Voltage in Volts
f_0 = Carrier Frequency in Hz
P_0 = Carrier Power in dBm
f_{+1} = First Upper Sideband Frequency in Hz
L_{+1} = First Upper Sideband Power in dBm
f_{-1} = First Lower Sideband Frequency in Hz
L_{-1} = First Lower Sideband Power in dBm
Γ = Calculated Acceleration Sensitivity in g^{-1}

Figure 16: Results of the acceleration sensitivity tests on the VCO for vibration frequency of 990 Hz. The spectrum analyzer span was 3960 Hz.
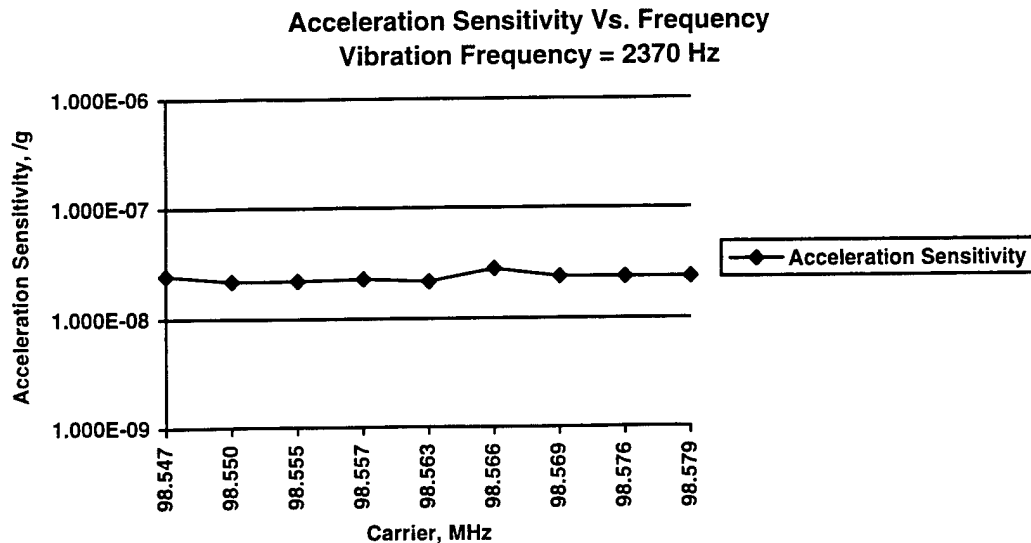
Acceleration Sensitivity Vs. Frequency
Vibration Frequency = 2370 Hz

Data:

V_{tune}	f_0	P_0	f_{+1}	L_{+1}	f_{-1}	L_{+1}	Γ
1.871	98 547 089	-6.20	98 549 463	-71.50	98 544 696	-72.60	2.453×10^{-8}
2.921	98 550 047	-5.90	98 552 468	-72.30	98 547 636	-73.10	2.198×10^{-8}
4.26	98 555 008	-4.10	98 557 401	-70.80	98 552 606	-70.80	2.224×10^{-8}
4.61	98 557 084	-3.80	98 559 484	-70.00	98 554 722	-70.40	2.302×10^{-8}
4.97	98 563 027	-4.60	98 565 410	-70.90	98 560 672	-72.10	2.173×10^{-8}
5.22	98 566 087	-5.30	98 568 451	-70.10	98 563 695	-69.80	2.815×10^{-8}
5.37	98 569 200	-6.00	98 571 602	-72.20	98 566 806	-71.90	2.396×10^{-8}
5.50	98 576 001	-8.00	98 578 381	-74.20	98 573 584	-74.00	2.382×10^{-8}
5.61	98 579 070	-8.60	98 581 407	-75.20	98 576 743	-74.30	2.369×10^{-8}

Key:

V_{tune} = Tuning Voltage in Volts
f_0 = Carrier Frequency in Hz
P_0 = Carrier Power in dBm
f_{+1} = First Upper Sideband Frequency in Hz
L_{+1} = First Upper Sideband Power in dBm
f_{-1} = First Lower Sideband Frequency in Hz
L_{-1} = First Lower Sideband Power in dBm
Γ = Calculated Acceleration Sensitivity in g^{-1}

Figure 17: Results of the acceleration sensitivity tests on the VCO for vibration frequency of 2370 Hz. The spectrum analyzer span was 9480 Hz.
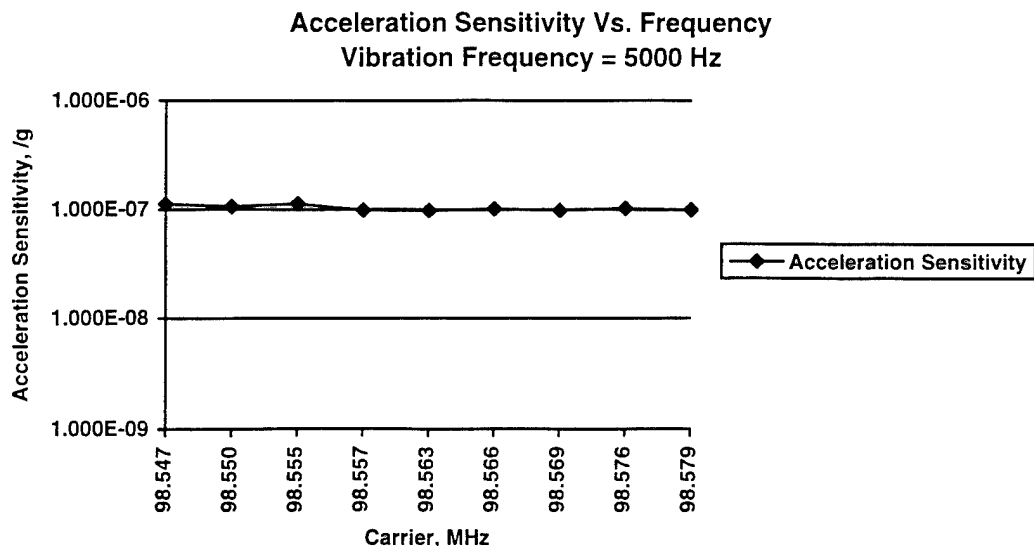
Acceleration Sensitivity Vs. Frequency
Vibration Frequency = 5000 Hz

Data:

V_{tune}	f_0	P_0	f_{+1}	L_{+1}	f_{-1}	L_{+1}	Γ
1.612	98 547 060	-5.90	98 552 100	-65.00	98 542 040	-65.00	1.126×10^{-7}
2.776	98 550 010	-5.90	98 555 040	-65.70	98 545 090	-65.30	1.073×10^{-7}
4.20	98 555 000	-3.80	98 560 160	-63.20	98 550 020	-62.40	1.138×10^{-7}
4.60	98 557 020	-3.40	98 562 060	-62.60	98 552 020	-64.70	9.859×10^{-8}
5.07	98 563 080	-3.90	98 568 220	-64.00	98 558 060	-64.50	9.745×10^{-8}
5.27	98 566 000	-4.40	98 571 000	-64.10	98 560 880	-64.60	1.020×10^{-7}
5.41	98 569 140	-5.80	98 574 220	-65.90	98 564 000	-66.40	9.744×10^{-8}
5.50	98 576 320	-8.00	98 581 440	-67.20	98 571 220	-68.60	1.026×10^{-7}
5.61	98 579 020	-8.50	98 584 000	-68.00	98 573 860	-69.30	9.970×10^{-8}

Key:

V_{tune} = Tuning Voltage in Volts
f_0 = Carrier Frequency in Hz
P_0 = Carrier Power in dBm
f_{+1} = First Upper Sideband Frequency in Hz
L_{+1} = First Upper Sideband Power in dBm
f_{-1} = First Lower Sideband Frequency in Hz
L_{-1} = First Lower Sideband Power in dBm
Γ = Calculated Acceleration Sensitivity in g^{-1}

Figure 18: Results of the acceleration sensitivity tests on the VCO for vibration frequency of 5000 Hz. The spectrum analyzer span was 20 kHz.

Table 1: Summary of measurements of the IN936B diodes.

Measurements on Tektronix Type 576 Curve Tracer:

Breakdown Voltage = -12.0 volts
Threshold Voltage = 0.5 volts

Results from Three-Stage Phase Shifter Test of the IN936B Diodes:

Tuning Voltage Range:	0.1 volts to 11 volts
Phase Change:	0^0 to 237^0
Sensitivity:	21.74^0 / volts
Maximum loss:	-3.5 dB

Tuning Volts	Phase in Degrees	Phase Change in Degrees	S_{21} in dB
0.100	-179	0	-1.0
0.500	-153	26	-1.0
1.000	-132	47	-1.2
2.000	-101	78	-1.6
3.000	-79	100	-1.7
4.000	-60	119	-1.8
5.000	-43	136	-1.7
6.000	-27	152	-1.7
7.000	-10	169	-1.6
8.000	7	186	-1.6
9.000	24	203	-2.0
10.000	42	221	-2.6
11.000	58	237	-3.5

Table 2: Gains and losses of the components of the VCO.

Component	$|S_{21}|$ in dB
3 cascaded MAR-6 amplifiers:	+53.8
ARL/PSD SAW-1:	-10.0
3 Stage Phase Shifter:	- 3.0
Power Divider:	- 3.0
Attenuators:	-35.0
Total Loop Gain:	2.8 dB

Table 3: VCO output in dBm versus frequency. Frequencies shown in bold type are those at which the transverse mode behavior on the SAW resonator had been measured. (See Figure 9 for the plot of output versus frequency.)

Tuning Volts, V_{tune}	Frequency, MHz	Output, dBm
-0.828	98.3873	-26.80
-0.503	98.3923	-14.70
-0.302	98.3985	- 7.70
-0.142	98.4090	- 4.70
-0.024	98.4261	- 7.80
0.0	98.4385	- 9.10
+0.034	98.4507	-10.00
+0.108	98.5002	- 8.70
+0.146	98.5138	- 7.10
+0.388	98.5334	- 3.90
+1.541	**98.5470**	- 6.10
+2.637	**98.5500**	- 6.10
+4.130	**98.5550**	- 4.10
+4.520	**98.5570**	- 3.70
+4.820	98.5603	- 4.60
+4.940	**98.5630**	- 4.70
+5.190	**98.5661**	- 4.70
+5.350	**98.5691**	- 5.90
+5.450	98.5730	- 7.70
+5.480	**98.5760**	- 8.20
+5.580	**98.5791**	- 8.60
+5.810	98.5886	-11.70
+5.930	98.5981	-14.70
+5.970	98.6098	-18.10
+6.040	98.6160	-20.00
+6.110	98.6375	-26.00
+6.120	98.6413	-27.50

Defense Technical Information Center*
ATTN: DTIC-OCC
Cameron Station (Bldg 5)
Alexandria, VA 22304-6145
(*Note: Two DTIC copies will be sent
from STINFO office, Ft Monmouth, NJ)

Director
US Army Material Systems Analysis Actv
ATTN: DRXSY-MP
(1)   Aberdeen Proving Ground, MD 21005

Commander, AMC
ATTN: AMCDE-SC
5001 Eisenhower Ave.
(1)   Alexandria, VA 22333-0001

Director
Army Research Laboratory
ATTN: AMSRL-D (John W. Lyons)
2800 Powder Mill Road
(1)   Adelphi, MD 20783-1197

Director
Army Research Laboratory
ATTN: AMSRL-DD (COL Thomas A. Dunn)
2800 Powder Mill Road
(1)   Adelphi, MD 20783-1197

Director
Army Research Laboratory
2800 Powder Mill Road
Adelphi, MD 20783-1145
(1) AMSRL-OP-SD-TA   (ARL Records Mgt)
(1) AMSRL-OP-SD-TL   (ARL Tech Library)
(1) AMSRL-OP-SD-TP   (ARL Tech Publ Br)

Directorate Executive
Army Research Laboratory
Physical Sciences Directorate
Fort Monmouth, NJ 07703-5601
(1) AMSRL-PS
(1) AMSRL-PS-T (M. Hayes)
(1) AMSRL-OP-FM-RM
(22) Originating Office

Advisory Group on Electron Devices
ATTN: Documents
Crystal Square 4
1745 Jefferson Davis Highway, Suite 500
(2) Arlington, VA 22202

Commander, CECOM
R&D Technical Library
Fort Monmouth, NJ 07703-5703
(1) AMSEL-IM-BM-I-L-R (Tech Library)
(3) AMSEL-IM-BM-I-L-R (STINFO Ofc)

Deputy for Science & Technology
Office, Asst Sec Army (R&D)
(1)   Washington, DC 20310

HQDA (DAMA-ARZ-D/
Dr. F.D. Verderame)
(1)   Washington, DC 20310

Director
Naval Research Laboratory
ATTN: Code 2627
(1)   Washington, DC 20375-5000

USAF Rome Laboratory
Technical Library, FL2810
ATTN: Documents Library
Corridor W, STE 262, RL/SUL
26 Electronics Parkway, Bldg 106
Griffiss Air Force Base
(1)   NY 13441-4514

Dir, ARL Battlefield
Environment Directorate
ATTN: AMSRL-BE
White Sands Missile Range
(1)   NM 88002-5501

Dir, ARL Sensors, Signatures,
Signal & Information Processing
Directorate (S3I)
ATTN: AMSRL-SS
2800 Powder Mill Road
(1)   Adelphi, MD 20783-1197

Dir, CECOM Night Vision/
Electronic Sensors Directorate
ATTN: AMSEL-RD-NV-D
(1)   Fort Belvoir, VA 22060-5677

Dir, CECOM Intelligence and
Electronic Warfare Directorate
ATTN: AMSEL-RD-IEW-D
Vint Hill Farms Station
(1)   Warrenton, VA 22186-5100

Cdr, Marine Corps Liaison Office
ATTN: AMSEL-LN-MC
(1)   Fort Monmouth, NJ 07703-5033